Article

Membrane fluidity, composition, and charge affect the activity and selectivity of the AMP ascaphin-8

Adriana Morales-Martínez,[1] Brandt Bertrand,[1] Juan M. Hernández-Meza,[1] Ramón Garduño-Juárez,[1] Jesús Silva-Sanchez,[2] and Carlos Munoz-Garay[1,*]

[1]Instituto de Ciencias Físicas, Universidad Nacional Autónoma de México (ICF-UNAM), Cuernavaca, Morelos, México and [2]Centro de Investigación sobre Enfermedades Infecciosas, Instituto Nacional de Salud Pública, Cuernavaca, Morelos, México

ABSTRACT   Ascaphins are cationic antimicrobial peptides that have been shown to have potential in the treatment of infectious diseases caused by multidrug-resistant pathogens (MDR). However, to date, their principal molecular target and mechanism of action are unknown. Results from peptide prediction software and molecular dynamics simulations confirmed that ascaphin-8 is an alpha-helical peptide. For the first time, the peptide was described as membranotrophic using biophysical approaches including calcein liposome leakage, Laurdan general polarization, and dynamic light scattering. Ascaphin-8's activity and selectivity were modulated by rearranging the spatial distribution of lysine (Var-K5), aspartic acid (Var-D4) residues, or substitution of phenylalanine with tyrosine (Var-Y). The parental peptide and its variants presented high affinity toward the bacterial membrane model ($\leq 2 \ \mu M$), but lost activity in sterol-enriched membranes (mammal and fungal models, with cholesterol and ergosterol, respectively). The peptide-induced pore size was estimated to be >20 nm in the bacterial model, with no difference among peptides. The same pattern was observed in membrane fluidity (general polarization) assays, where all peptides reduced membrane fluidity of the bacterial model but not in the models containing sterols. The peptides also showed high activity toward MDR bacteria. Moreover, peptide sensitivity of the artificial membrane models compared with pathogenic bacterial isolates were in good agreement.

SIGNIFICANCE   The antimicrobial peptide ascaphin-8 has potential for clinical applications but has barely been studied. Until now, the cellular target of this peptide and its mechanism of action were unknown. Biophysical characterization, including molecular dynamics, fluorescence spectroscopy and dynamic light scattering, revealed that ascaphin-8 is an alpha-helical membranotrophic peptide. The factors that govern peptide activity and specificity were elucidated by designing variants with different charge distribution, and effect of the volume of aromatic residues. This work exemplifies the urgent need to describe the physicochemical properties of peptides as well as the physical properties of membranes targets. Understanding peptide interaction with different membranes provides useful information for the rational design of antimicrobial peptides that can be used as antibiotics.

INTRODUCTION

The emergence of multidrug-resistant (MDR) pathogens, such as *Enterococcus faecium*, *Staphylococcus aureus*, *Klebsiella pneumoniae*, *Acinetobacter baumannii*, *Pseudomonas aeruginosa*, and *Enterobacter* species, among others, has been one of the most urgent global problems over the last couple of decades, putting enormous strain on the health

sector (1). It is estimated that over 700,000 patients die worldwide due to infections caused by these MDR pathogens and that the death toll could increase to approximately 10 million by the year 2050 (2). Moreover, the decline in the approval of new antibiotics and the use of drugs with toxic side effects have further aggravated the estimated morbidity and mortality rates (3,4).

Currently, major alternatives to conventional antibiotics that could mitigate this growing health crisis include phage technologies, lysins, bacteriocins CRISPR/Cas9, probiotics, innate defense regulatory peptides, antibodies, and antimicrobial peptides (AMPs) (synthetic mimics or natural); each with their respective advantages and disadvantages (see Ghosh et at. 2018 (2), for further information).

Over the years, AMPs have become an attractive alternative to design efficient new antibiotics to fight infectious diseases caused by MDR pathogens due to their broad spectrum of microbicidal activity (5) and because of the low probability of MDR strains of developing resistance (4). In fact, they have been referred to as promising next-generation antibiotics (3). The global peptide therapeutics was valued at around 39 billion USD in 2021 and is expected to grow at a compound annual growth rate of 6.4% for the rest of the decade, according to a new report by Grand View Research. However, despite significant progress, only about 60 synthetic therapeutic peptides have reached American, European, or Japanese pharmaceutical markets, but several hundreds of novel therapeutic peptides are in preclinical and clinical development (6).

AMPs are important effector molecules ubiquitous in nature that evolved over millions of years as the first line of defense against invading pathogens (5). These biomolecules are amphipathic in nature and are usually less than 50 amino acids in length (7). Although anionic AMPs have been reported (8,9), the most studied AMPs are cationic in nature due to the electrostatic interactions they establish with their negatively charged target membranes in the initial stage of membrane disruption (10,11). Cationic AMPs assume four general amphiphilic conformations: 1) either disordered structures that form alpha-helix conformers on interaction with target membranes, 2) beta-sheets stabilized by disulfide bridges, 3) cyclic structures, or 4) a more extended conformation (12,13).

AMPs have a wide range of mechanisms, ranging from intracellular targets (inhibiting protein synthesis, protein folding, or enzymatic activity) to disruptive effects on the cell wall and membrane (14). AMPs that kill microorganisms via receptor-mediated membrane damage are not of great interest since resistance is generally generated by mutations that lead to resistant phenotypes (15,16). On the other hand, AMPs that target cell membranes act through numerous mechanisms of pore formation (barrel stave, toroidal pore, etc.) or general disruption (detergent-like activity), finally resulting in lysis and cell death, are promising and attractive, because resistance is less likely to occur (17).

Frog skin secretions are among the richest sources of naturally occurring AMPs belonging to different families, with more than 1000 registered AMPs in the Antimicrobial Peptide Data Base over 18 years. Thus, AMPs from amphibians have gained a lot of interest especially in the discovery, structure-function characterization, and development of novel compounds to combat antimicrobial resistance (18).

The family of cationic AMPs known as ascaphins (numbered 1 to 8) was first discovered in skin secretions of *Ascaphus truei* and described in 2004 (19). Ascaphins present high activity toward clinically relevant microbial species, such as *K. pneumoniae*, *S. aureus*, *E. faecalis*, *P. aeruginosa*, *Escherichia coli*, *Enterobacter cloacae*, *Proteus mirabilis*, *Staphylococcus epidermidis*, *Streptococcus* group B, *Serratia marcescens*, *Citrobacter freundii*, *Salmonella* sp., *Shigella flexneri*, and *Candida albicans*. They show varying but generally high cytotoxic activity against human erythrocytes, with ascaphin-8 being the most hemolytic (19,20).

Although phylogenic analyses have revealed the evolutionary history of the ascaphins and their effectiveness against pathogenic strains have been well documented, their principal target and mechanism of action have not been explored previously. Based on sequence homology to other frog skin AMPs and biochemical properties, the current hypothesis suggests that the ascaphins most likely induce cell lysis through membrane disruption (19). To our knowledge, this is the first study that experimentally demonstrates that the main target of this family of peptides is the cell membrane.

Here, ascaphin-8 is described as an alpha-helical membranotrophic AMP that disrupts cell membranes by pore formation and affects membrane fluidity. In addition, the activity and specificity of ascaphin-8 were tuned through semirational peptide design, increasing its specificity toward bacterial cell membranes while theoretically reducing its hemolytic index. The results and conclusions of the artificial membrane models used and pathogenic bacterial isolates in terms of peptide sensitivity were in good agreement.

MATERIALS AND METHOD

Reagents

High purity calcein was purchased from Invitrogen (Life Technologies, Eugene, OR). High purity fluorescein isothiocyanate (FITC)-dextran 20, 70, 150, 250, and 500 kDa were purchased from Sigma Aldrich (Merck KGaA, Darmstadt, Germany). High purity Laurdan (6-dodecanoyl-2-dimethylaminonaphthalene) was purchased from Cayman Chemical. Fluospheres Size kit 2, carboxylate, yellow-green (505/515) (Molecular Probes) were purchased from Life Technologies (Eugene, Oregon, USA). N-(2-Hydroxyethyl) piperazine-N′-(2-ethanesulfonic acid) (HEPES), potassium chloride, potassium hydroxide, sodium chloride, calcium chloride, 4-(1,1,3,3-tetramethylbutyl)phenyl-polyethylene glycol (Triton X-100), benzyl alcohol (BA), and ergosterol (ERG) were purchased from Sigma Aldrich (Merck KGaA). Phospholipids 1-palmitoyl-2-oleoyl-*sn*-glycero-3-phosphocholine (POPC), 1-palmitoyl-2-oleoyl-*sn*-glycero-3-phospho-(1′-*rac*-glycerol) (POPG), and cholesterol (CHL) were purchased from Avanti Polar Lipids (Alabaster, AL). Chloroform was purchased from JT Baker, Thermo Fisher Scientific (Waltham, MA). Sephadex G-75 was purchased from Pharmacia Fine Chemicals, Division of Pharmacia (Piscataway, NJ). The peptides were synthesized, purified, and shipped by GenScript (Piscataway, NJ, USA).

Prediction of biochemical properties

Ascaphin-8 (GFKDLLKGAAKALVKTVLF) was retrieved from the AMP data base (https://aps.unmc.edu/), and its biochemical characteristics were predicted with https://pepcalc.com/, https://www.peptide2.com/N_peptide_hydrophobicity_hydrophilicity.php, https://ciencias.medellin.unal.edu.co/gruposdeinvestigacion/prospeccionydisenobiomoleculas/InverPep/public/typep_en, http://www.camp3.bicnirrh.res.in/predict/, and http://www.gravy-calculator.de/.

Structure prediction and molecular dynamics simulations

Maximin 3 6HZ2 (retrieved from the Protein Data Bank) was used as a reference structure to predict the structure of ascaphin-8. The missing protons from the NMR-resolved structure were added using Scwrl4 software (http://dunbrack.fccc.edu/SCWRL3.php/). Pep-fold 3 (https://mobyle.rpbs.univ-paris-diderot.fr/cgi-bin/portal.py#forms::PEP-FOLD3) was used to generate models of maximin 3 and ascaphin-8. The model's structure minimization was carried out in Pep-fold 3 (21) and Chimera (22). PyMOL (23) was used for root mean-square deviation calculations and structure visualization. The predicted structure of ascaphin-8 was studied in two environments, in aqueous solution and embedded in the membrane. Both systems were mounted aided by the input generator in CHARMM-GUI's web service (24,25,26,27,28). Then molecular dynamics (MD) simulations were run in GROMACS 2021.2 (29) using the CHARMM36m force field (30) at 303.15 K with separate couplings for the solute (peptide) and solvent. The time step used for the leap-frog integrator was 2 fs; the hydrogen movement was constrained with the LINCS algorithm (29), and the PME was used with a cutoff of 1.2 nm. For the experiment in aqueous solution, a single ascaphin-8 peptide molecule was inserted into a triclinic cell with initial dimensions of $9 \times 9 \times 8$ nm^3, with 3976 TIP3P water molecules, 11 sodium ions, 1 calcium ion, and 16 chloride ions. After minimizing the water-peptide system using the steepest descend algorithm, 30 ns of NVT equilibration were performed, and the Berendsen thermostat (31) was used with a time constant of 0.2 ps.

For the membrane environment, ascaphin-8 was embedded in a bilayer composed of 240 POPC lipid molecules, 120,000 TIP (water molecules), 27 sodium ions, calcium ions, and 38 chloride ions. The dimensions of the simulation box were $9 \times 9 \times 8$ nm^3. The system was minimized, and two NPT equilibrations were run. All production stages were carried out with the NPT ensemble, using semi-isotropic coupling with Parrinello-Rahman (32) ($p = 0.2$ fs) and Nose-Hoover thermostat (33,34) (t = x) for 500 ns, with four replicas. MD simulations were analyzed using GROMACS (29) and VMD (35). The MD system parameters were plotted using GraphPad Prism 9. The VMD-SS plugin was used for secondary structure analysis (36).

3-D hydrophobic moment

Snapshots in both simulations (in solution and embedded in the POPC bilayer) were taken from the initial structural conformations and every 100 ns (i.e., a total of six snapshots). The average HM vector and the angle between HM were calculated with the 3D Hydrophobic Moment Vector Calculator (https://www.ibg.kit.edu/HM) (37).

Biophysical characterization

Liposome preparation and leakage experiments

To study the action of peptides that promote calcein leakage from the vesicle's internal compartment, large unilamellar vesicles (LUVs) of POPC:POPG (80:20), POPC:CHL (70:30), and POPC:ERG (70:30), with encapsulated calcein were prepared. The LUVs were assembled by hydrating a dried lipid film with 150 μL of an 80 mM calcein solution, 70 mM KCl/10 mM HEPES buffer (pH 7.2). This was followed by vortexing for 5 min at constant high speeds, hydration for 10 min in a water bath at 40°C, and finally passed by extrusion with 100 nm pore size filters. Untrapped calcein was separated from the LUVs by size-exclusion chromatography in a Sephadex-G75 column (Pharmacia Fine Chemicals) using the KCl buffer. Calcein release from the LUVs was monitored by adding increasing concentrations (0.0015–10 μM) of peptide until saturation to LUVs in a glass round cuvette under agitation in 150 mM NaCl/2.5 mM CaCl$_2$/10 mM HEPES buffer (pH 7.2). Calcein fluorescence was measured at 520 nm after excitation at 490 nm in an AMINCO-Bowman Series 2 Luminescence Spectrometer (Wisconsin,USA). The percentage of leakage was determined according to Eq. 1:

$$\text{Leakage} = \frac{[F - F_0]}{[F \max - F^0]} \times 100. \qquad (1)$$

The maximum fluorescence intensity (F_{max}) was determined by adding Triton X-100 with a final concentration of 0.05% (v/v) to the cuvette; F_0 represents the initial fluorescence intensity of the intact vesicle, and F the intensity after incubation with the peptide. Like the calcein leakage assays, liposome leakage assays to estimate pore size induced by the peptides FITC-dextran (40, 70, 250, and 500 kDa at 50 mg mL^{-1}) were carried out. At least three independent experiments were performed. Dose-response curves were drawn, and the effective concentration (EC) values, EC$_{20}$, EC$_{50}$, and EC$_{80}$, were calculated using OriginPro 8.

Effect of peptides on membrane fluidity

Changes in penetration and mobility of water in the membrane models were analyzed employing Laurdan-generalized polarization (GP) developed by Parasassi et al. (38). GP was determined as described by Scheinpflug et al. (39). In brief, POPC:POPG (80:20), POPC:CHL (70:30), and POPC:ERG (70:30) Laurdan stained liposomes were prepared in a ratio of 1.5:1000 (dye/lipid). Fluorescence measurements were carried out using an AMINCO-Bowman Series 2 Luminescence Spectrometer with a fixed excitation at 350 nm, and two emission wavelengths at 435 and 500 nm were recorded. Liposome solutions (2 μM) were used, and measurements were taken in 5 s intervals for 100 s and averaged. Each experiment consisted of three to six replicas, and at least three independent experiments were carried out. The system was validated by measuring the GP of different liposomes in the presence of 10% (v/v) BA, the latter being a membrane fluidizer. The temperature was controlled by an H145092 Brinkmann LAUDA Rm6 Recirculating Water Bath/chiller RMT6. Afterward, the effect of the peptides on GP was evaluated at the respective EC$_{80}$ value calculated for each peptide from the calcein leakage experiments. GP was calculated according to Eq. 2:

$$\text{GP} = \frac{[I_{435} - I_{500}]}{[I_{435} + I_{500}]}. \qquad (2)$$

Dynamic light scattering and aggregation prediction

Dynamic light scattering (DLS) measurements were carried out with a Malvern Zetasizer Nano ZS (Malvern, Herrenberg, Germany) equipped with a 633 nm He-Ne laser and operating at an angle of 90°. The parameters used were viscosity = 0.8926 cp and refractive index of NaCl/HEPES buffer = 1.3717. The samples were analyzed in plastic cuvettes at 25°C using the automatic mode for identifying the best number of subruns and measurement time (n = 10). The z-average radius (Z average) and polydispersity index were calculated from the correlation function using Dispersion Technology Software version 6.01 (Malvern) (40). The buffer applied in the calcein leakage experiments (150 mM NaCl, 2.5 mM CaCl$_2$/10 mM HEPES buffer [pH 7.2]) was also used for particle size determination. Fluospheres Size kit 2, carboxylate, yellow-green (505/515) 20, 100, 200, 500, and 1000 nm standards (Molecular Probes by Life Technologies) were used as size standards. For the hydrodynamic radius determination of the peptides, the same concentrations as those employed in the calcein release experiments were used. The error bars displayed on the DLS graphs were obtained by the standard deviation of at least three independent experiments. The peptides' theoretical volumes were estimated using the peptide property calculator from the Center for Biotechnology Northwestern University Evanston, IL (http://biotools.nubic.northwestern.edu/proteincalc.html). Also, the effect of ascaphin-8 and its variants on liposome size was evaluated.

In addition, the AGGRESCAN 3D 2.0 server (https://ciencias.medellin.unal.edu.co/gruposdeinvestigacion/prospecciondisenobiomoleculas/InverPep/public/tools) and the PASTA 2.0 (http://old.protein.bio.unipd.it/pasta2/)

platforms were used to estimate the aggregation tendencies of ascaphin-8 and its variants (41).

Antimicrobial activity assays

Initially, the antibacterial activity of the peptides was qualitatively measured following the Kirby-Bauer method (1996) (42), according to the Clinical and Laboratory Standards Institute recommendations. In brief, petri dishes containing Müeller-Hinton agar were sown with bacteria inoculums from 1 to 2×10^8 colony-forming units/mL. Then, 3 μL (2 μg/μL) corresponding to 6, 0.6, and 0.06 μg of peptide solution was placed over the agar; these concentrations were equivalent to 999, 99, and 9 μM. Incubation time was from 16 to 19 h at 35 ± 2°C. A halo of growth inhibition was observed as a positive result. Antimicrobial assays were carried out against two susceptible strains: *E. coli* ATCC 25922 (Gram-negative), and *S. aureus* ATCC 29213 (Gram-positive); and MDR clinical isolates: *E. coli* 10225, *A. baumannii* 10324, *K. pneumoniae* 6411, *P. aeruginosa* 4899 and 4677, and *P. rettgerii*, 06-1619.

RESULTS AND DISCUSSION

Design of ascaphin-8 variants

Potent antimicrobial activity is generally accompanied by excessive cytotoxicity toward host cells; therefore, modifying native peptide sequences based on desirable biophysical properties can help tune the activity and selectivity of promising AMP candidates (4,43). Three variants of ascaphin-8 were designed to evaluate the structure-activity relationship, i.e., tune activity and selectivity. The following ascaphin-8 variants were designed, modeled (using the ascaphin-8 structure as a template), and synthesized by GenScript: 1. K3L/L5K (or Var-K5) variant-GFLD**K**LKG AAKALVKTVLF, where lysine (K3) was switched with leucine (L5). G1D/D4G (or Var-D4) variant-**D**FKGLL KGAAKALVKTVLF, where aspartate (D4) position was switched with glycine (G1). 3. F2Y,F19Y (or Var-Y) variant-G**Y**KDLLKGAAKALVKTVL**Y**, where phenylalanine F2 and F19 were substituted by tyrosine (Y). The multiple alignment of the peptide sequences is presented in Fig. 1, and the predicted biochemical properties are presented in Table 1. The predicted structures are presented in Fig. 2.

The models were consistent with the predictions carried out in AlphaFold, which is a machine learning-based predictor. Important to note is that AlphaFold is the most reliable

Maximin 3	GIGGKILSGLKTALKGAAKELASTYLH	27
Ascaphin-8	-------GFKDLLKGAAKALVKTVLF	19
Var-K5	-------GFLDKLKGAAKALVKTVLF	19
Var-D4	-------DFKGLLKGAAKALVKTVLF	19
Var-Y3	-------GYKDLLKGAAKALVKTVLY	19

FIGURE 1 Multiple alignment of maximin-3 (used as the reference structure 72.7% identity), ascaphin-8 and Var-K5 (K3L; L5K), Var-D4 (G1D; D4G), and Var-Y (F2Y; F19Y) using the Clustal Omega server (https://www.ebi.ac.uk/Tools/msa/clustalo/). Letters underlined in black indicate the residues that were modified compared with the parental ascaphin-8 sequence. To see this figure in color, go online.

protein structure predictor available since its predictions are basically indistinguishable from those determined using experimental methods, such as x-ray crystallography and, in recent years, cryoelectron microscopy (44,45) (Fig. S1).

The charge distribution of cationic peptides has been proven to be an important factor in AMP activity (14,46,47). Ascaphin-8 has all its lysine residues on one face on the peptide's surface; thus, the Var-K5 variant was designed so that the first lysine residue in its primary structure would be on the opposite surface of the other three lysines (Fig. 2 *A*, I and II). The hypothesis is that the membrane affinity of the peptide would be modified since charge distribution plays an essential role in the initial electrostatic interaction between the peptide and the membrane surface (15). The effect of the distribution of lysine residues has been reported elsewhere (20,46). For instance, Eley et al. (20) assessed a series of L-lysine substituted ascaphin-8 analogs against a range of clinical isolates of extended-spectrum β-lactamase-producing Gram-negative bacteria. The authors were able to fine-tune antimicrobial activity and selectivity, improve activity, and reduce hemolytic activity in some cases of the parental peptide. In the case of Pandinin 2 (Pin2) and Pin2[GVG] where, apart from other notable structural differences, the lysine distribution is different. The Pin2[GVG] variant AMP has all its lysine residues on one face of the structure, while the Pin2 has one lysine residue on the opposite side of the structure (48,49). The overall structural differences between both peptides result in higher activity (and similar dose-response curves) and less specificity (different dose-response curves) of Pin2[GVG] compared with Pin2 (11). In this work, we were careful not to drastically modify other parameters, such as hydrophobicity and solubility; although the HM was slightly modified.

In the case of the Var-D4 variant, we were interested in the position of the aspartic acid. So far, the implication of this amino acid has not been considered for modulating AMP activity and selectivity. Here, the hypothesis planted was similar to the Var-K5 variant lysine distribution. As can be observed from the multiple alignment of the peptides (Fig. 1), the four lysine residues in the ascaphin-8 parental primary structure seem to be interrupted by the aspartic acid (D) residue at position 4 (K3, **D4**, K7, K11, K15). This residue was moved to position 1 in the peptide sequence (**D1**, K3, K7, K11, K15), forming a positive continuous primary structure. As with the Var-K5 variant, the predicted biochemical properties of the peptide were not modified.

Var-Y was designed by substituting phenylalanine with tyrosine at positions 2 and 19. Tyrosine with a hydroxyl group at the aromatic ring is enriched at interfacial regions of membrane proteins; thus, peptides with this residue may remain on the surface of the zwitterionic membrane in mammalian cells. However, a peptide containing tyrosine may be transferred into the inner leaflet of the bacterial

TABLE 1 Predicted biochemical properties of maximin 3 and ascaphin-8 and its variants

Peptide	No. of residues	mW (Da)	Net charge	pI	Hydrophob.	GRAVY	Sol. in water	HM (A*kT/e)	Angle (θ)	SVM
Maximin 3	27	2698.17	3.1	10.42	0.24	0.24	poor	22.14	20.20	0.960
Ascaphin-8	19	2019.47	3.0	10.70	0.74	0.73	good	11.73	49.04	0.990
Var-K5	19	2019.47	3.0	10.70	0.74	0.73	good	9.143	75.08	0.982
Var-D4	19	2019.47	3.0	10.71	0.74	0.73	good	11.03	106.59	0.937
Var-Y	19	2051.47	3.0	10.22	0.31	0.30	good	11.18	102.13	0.946

Hydrophob., hydrophobicity; Sol., solubility; GRAVY, grand average of hydropathicity; (AkT/e), 3D hydrophobic moment; Angle, angle between HM vector and z axis; SVM, support vector machines classifier.

membrane, which contains phosphatidylglycerol with a negatively charged headgroup, with the effect of positively charged lysine residues in the structure (50). Moreover, the presence of tyrosine can be exploited by fluorescence-quenching studies due to its intrinsic fluorescence properties, which is a valuable tool for quantifying their insertion into the lipid membranes (51). Therefore, the hypothesis here is that this variant should also show specificity toward bacterial cells and should present less cytotoxicity toward erythrocytes, improving its therapeutic index. Another reason for designing this variant was that preliminary results in our laboratory suggest that tyrosine may affect the anchoring of peptides (in this case, lipopeptides) in POPC:ERG membrane models (unpublished data).

Prediction of biochemical properties

The exact relationships between the composition and properties of AMPs and the composition and properties of their target cell membranes are not well understood. A better understanding of the relationship between these two, is critical to designing novel molecules with increased potency and specificity (52). As observed in Table 1, the biochemical parameters of the peptides were basically unchanged, except for the hydrophobicity parameters (net hydrophobicity, aliphatic index, GRAVY, and hydrophobic moment [HM]) and the support vector machine (SVM) predictor values.

Algorithms, such as SVM, random forest, artificial neural network, and discriminant analysis, are useful tools for predicting the probability of amino acid sequences to present antimicrobial activity. The SVM model uses a simple descriptor of properties, such as amino acid content, charge, hydrophilicity, and polarity, to quantitatively predict antimicrobial activity (53). The closer the value is to 1, the higher the probability of the peptide to present antimicrobial activity. It is important to point out that this algorithm is only limited to predicting the probability of AMP activity but not its potency or selectivity (i.e., the preference toward Gram-positive, Gram-negative, fungal, or mammal cells
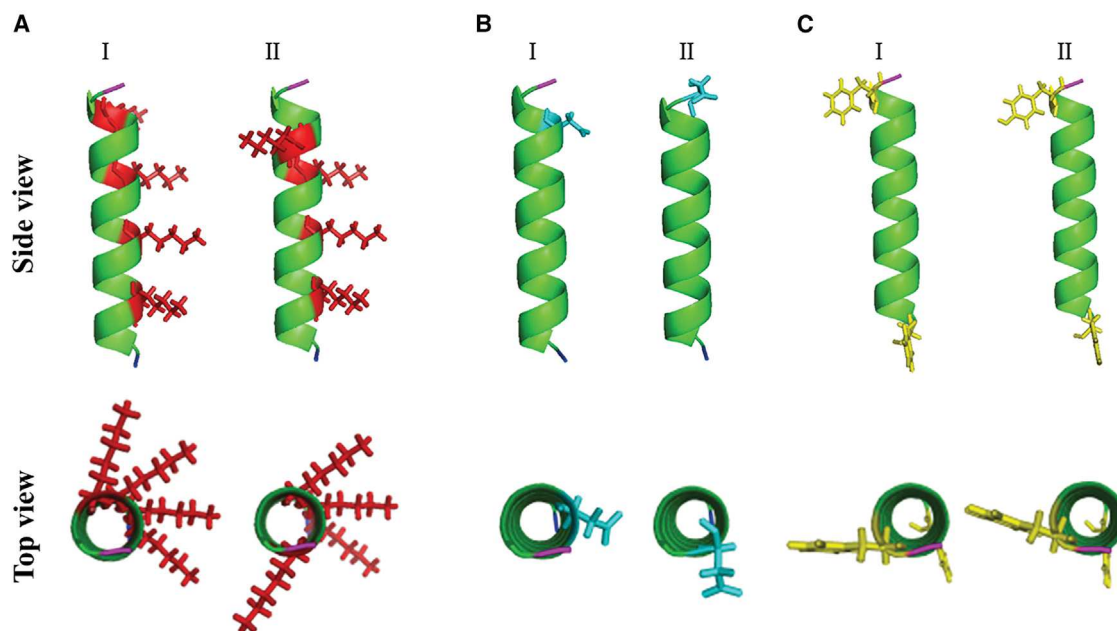
FIGURE 2 Illustrations of the side and top views of the predicted peptide structures. (A) I-ascaphin-8 compared with II-Var-K5 (lysine residues, *red*). (B) I-ascaphin-8 compared with II-Var-D4 (aspartate residues, *cyan*). (C) I-ascaphin-8 compared with II-Var-Y (phenylalanine or tyrosine residues, *yellow*). Magenta, N-terminal; blue, C-terminal. To see this figure in color, go online.

cannot be predicted). Here, ascaphin-8 presented the highest score, followed by Var-K5, Var-Y3, and Var-D4.

On the other hand, hydrophobicity (GRAVY, aliphatic index, solubility in water) is calculated by the sum of all the hydrophobic residues divided by the length of the peptide. Greater values indicate hydrophobicity, while lower values represent hydrophilic properties. Var-Y3 was predicted as the least hydrophobic peptide. This can be attributed to the fact that tyrosine is less hydrophobic than phenylalanine. AMPs typically contain approximately 50% hydrophobic residues. Studies have shown that increasing hydrophobicity to optimal percentage can increase activity against microbial cell membranes; however, further increasing the hydrophobicity beyond specific optimum point results in loss of antimicrobial activity and increased activity toward neutral membranes, which is related to mammalian cell toxicity (54,55). Another parameter that considers hydrophobicity is the HM. HM is considered as one of the most important properties used to predict AMP activity; a greater HM is generally related to increased activity. The HM is defined as the degree to which polar and nonpolar residues are segregated along the helix axis (the mean vector sum of the hydrophobicities of the amino acid side chains in a helical peptide (56). The 3D Hydrophobic Moment Vector Calculator predicts the angle between the 3D-HM vector and the helix axis of peptides (37). It is proposed that peptide activity is related to the equilibrium between surface-bound and inserted peptides, and that peptides that are more steeply tilted also have their equilibrium shifted more toward the inserted state and, therefore, are more active. In this case, hypothetically, if peptide activity and selectivity were not multifactorial and only depended on tilt angles, ascaphin-8 and maximin 3 could be predicted to be the most active. It is very important to point out that these predictors do not take into account membrane composition (i.e., differences between the POPC:POPC, POPC:CHL, or POPC:ERG used in this study) that could affect the tilt angles of peptides (47,57).

Hydrophobicity and solubility are closely related to peptide self-association or aggregation (i.e., the ability to oligomerize/dimerize) in an aqueous solution, a crucial parameter for antimicrobial activity (58). In this study, we used DLS, the Aggrescan 3D 2.0, and PASTA 2.0 platforms to study this phenomenon. AGGRESCAN was applied to calculate the aggregation propensities of amino acids derived from the experimental data of amyloid-beta peptides, and it resulted in a good predictor of the in vivo peptide aggregation phenomenon. PASTA 2.0 provides a versatile platform where different features can be easily predicted using input sequences. The server provides other pieces of information, such as intrinsic disorder and secondary structure predictions, that complement the aggregation data. The predicted aggregation propensities assume that the soluble form is natively unstructured (59). The assumption is particularly relevant since most cationic AMPs pre-

sent disordered structures in solution and only take on their helical structure on insertion into lipid membranes (15). The tendency of the peptides to aggregate is shown in Table S1. According to the aggregation tendency prediction, ascaphin-8 is most likely to aggregate, followed by Var-D4, Var-K5, and Var-Y3. Again, a limitation is that this server does not consider environmental conditions (i.e., aggregation in solution or aggregation/dimerization in the membrane/lipid environment). The aggregation tendency is related to the size of the peptide aggregates in solution, which has been shown to affect overall activity (i.e., the bigger the aggregates, the higher the activity) (11). However, these peptides' residues and regions to self-associate were also graphically analyzed (Figs. S3 and S4). In all cases, ascaphin-8 and its variants are prone to aggregate through the second half of the sequences (i.e., the C-terminal end). Var-Y is the least likely to aggregate based on aggregation prediction (probably due to its lower hydrophobic index) and, thus, suggests that it might just be the most membrane selective peptide. Peptide aggregation studies utilizing MD in solution and when in contact with lipid bilayers are currently being considered in our laboratory.

Structural behavior of ascaphin-8 in aqueous solution and in lipid bilayers by MD

MD simulations help study AMP folding. Since AMP activity often varies between different complex biological systems, carefully choosing the system at the molecular level is particularly relevant for understanding the mechanisms of action of AMPs (60). Thus, the experimental conditions (buffer solution) were simulated (NaCl and $CaCl_2$ at 150 and 2.5 mM, respectively). Experimental and theoretical studies show that many AMPs are partially or totally disordered in aqueous environments and fold into their functional secondary structures when interacting with the membrane-solvent surface (61). However, in the case of the ascaphin family, there are no experimental or theoretical reports on their structure. Understanding the behavior and structure stability of such peptides in an aqueous solution or the membrane environment could aid in understanding their mechanism of action. In this work we employed molecular dynamics to explore this particular topic. The results of the structural behavior of ascaphin-8 in solution and the POPC bilayer are shown in Fig. 3. The graphical representations were generated using the VMD-SS plugin that calculates the percentage secondary structure (y axis) of the peptide during the simulation (x axis) (36). The alpha-helix structure of ascaphin-8 previously predicted was used for studying the peptide folding dynamics.

In accordance with the predicted behavior of alpha-helical peptides, the organized structure was lost entirely after approximately 200 ns (in aqueous solution), in most cases. Alpha-helix structures are represented in blue dots and purple lines, and other structures, such as turns and extended
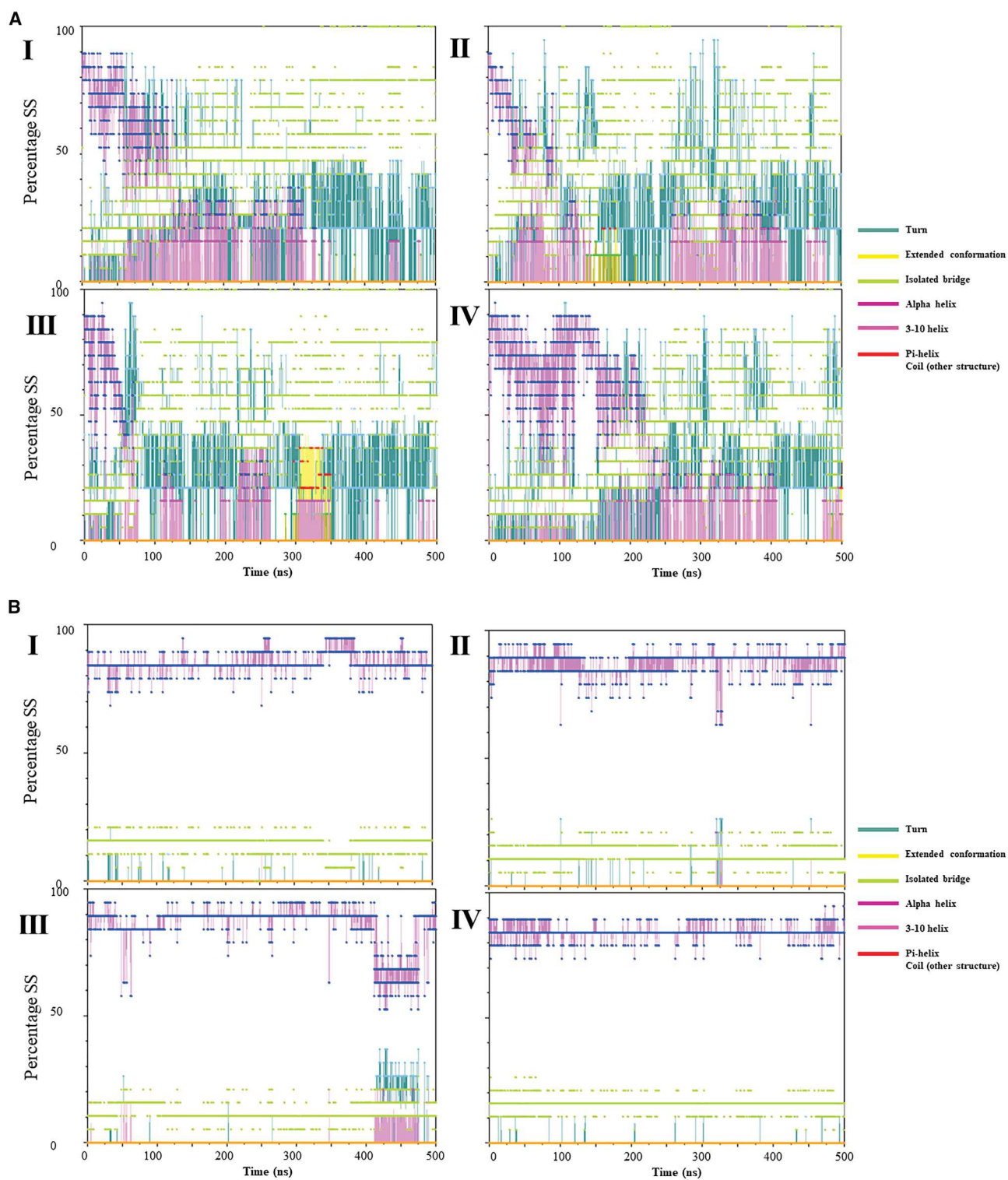
FIGURE 3 Structural behavior of ascaphin-8 in different environments. (*A*) Representation of the structural conformations of ascaphin-8 in solution during 500 ns. (*B*) Representation of the structural conformations of ascaphin-8 embedded in a POPC bilayer during 500 ns. I, II, III, and IV represent replicas of each experiment. Different colors represent the percentage of the different structural conformations of the peptide throughout the simulation. To see this figure in color, go online.

bridges, are represented by dark green lines and light green dots, respectively (Fig. 3 A). Ascaphin-8 presented a helicity of ~90% and 10% coil at the start of the simulations and dropped to ~30% and 70%, respectively, at the end of the simulation. Fig. 4 shows representative structural conformations of the peptide in aqueous solution at different sampling times (i.e., approximately every 100 ns), corroborating the structural information obtained in Fig. 3 A. On the other hand, ascaphin-8 showed slight structural variation throughout the simulation's membrane environment (Fig. 3 B). As in the case of the peptide in the aqueous solution experiment, initial helicity was 90% and dropped to ~86%, while coil structure was initially 10% and slightly increased to 13%. The number of hydrogen bonds (decreasing in number) of the peptide in aqueous solution,

and the constant number of hydrogen bonds of the peptide embedded in the bilayer (Fig. S5), were consistent with the structural behavior presented in Fig. 3 A. MD simulations of ascaphin-8 and its variants have been carried out by our laboratory in different membrane models, namely POPC:POPG, POPC:CHL, and POPC:ERG mimicking bacterial, mammal, and fungal membranes, respectively. The effect of these peptides on the aforementioned membrane models and lipid-peptide interaction will be published in a follow-up paper (manuscript in preparation).

In addition, the fluctuation in the absolute HM (A*kT/e) and the angle between the HM and the z axis (θ) of ascaphin-8 in solution and the POPC bilayer was also consistent with the structural behavior of the peptide. The HM and θ fluctuated notably in solution while being fairly
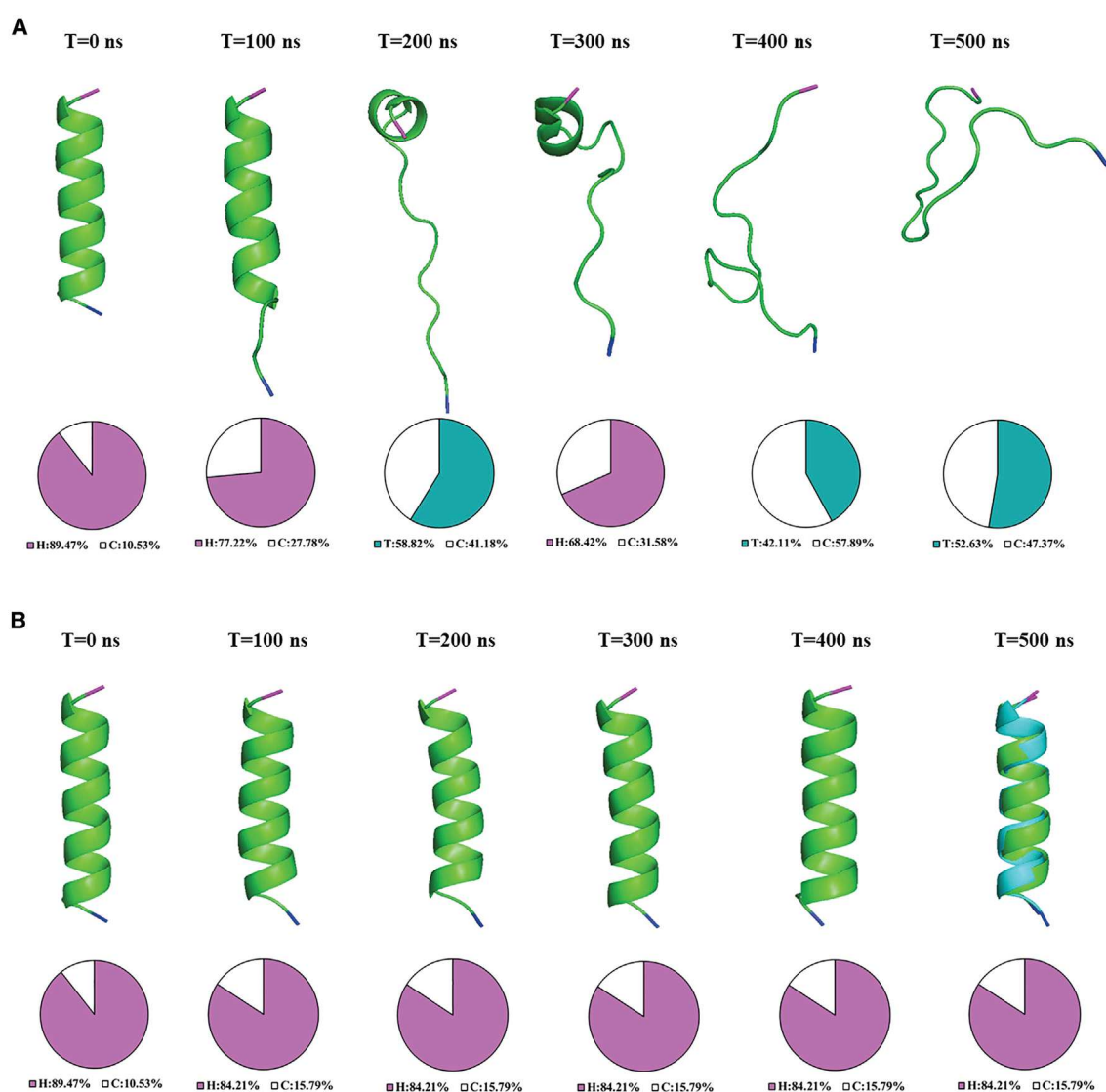

FIGURE 4 Snapshots of representative structures of ascaphin-8 in (A) aqueous solution and (B) in a POPC bilayer; T = 500 ns superimposition of T = 0 ns (*green*) with T = 500 ns (*cyan*). Magenta, N-terminal; blue, C-terminal. Pie charts represent the percentage of secondary structure of the illustrated snapshots (H, alpha helix; C, coil; T, turn). To see this figure in color, go online.

constant in the membrane environment (Fig. S6). This observation suggests that the estimated HM of the alpha-helical structure of ascaphin-8 is relevant for the interaction among momomers and membrane lipids.

Calcein leakage experiments

Cell membranes are extremely complex and dynamic structures that can be studied through lipid membrane models. Different membranes can be mimicked using representative lipids (most abundant lipids), making these systems popular choices for membrane-active peptide studies. On the other hand, the leakage of fluorescent molecules from liposomes is a golden standard for confirming dysregulation of membrane integrity. Liposome leakage experiments are used to identify membrane perturbation positively, but they do not give direct information on the type of membrane disturbance (i.e., type of pores formed or detergent-like activity) (62).

In this study, we prepared well-established archetypes of LUVs to mimic bacterial cells (POPC:POPG, 8:2), erythro-cytes (POPC:CHL, 7:3), and fungal cell membranes (POPC:ERG, 7:3) for studying the effect of ascaphin-8 as a membranotrophic agent. Our results are the first account to experimentally confirm the membrane activity of this peptide (Fig. 5).

Ascaphin-8 presented 100% activity toward the bacterial system and lost 80% of its activity in the erythrocyte system presenting EC_{50} values of 0.986 ± 0.159, 3.87 ± 1.10, and 3.54 ± 0.60 μM, for the bacterial, mammal, and fungal systems, respectively. Our EC_{50} values are comparable with the first report on the ascaphin family, where ascaphin-8 presented a minimum inhibitory concentration of 6 μM toward *E. coli* and *S. aureus*, while presenting a hemolytic concentration (HC_{50}) of 50 μM toward human erythrocytes (19), equivalent to a loss of activity of approximately 80% toward erythrocyte cells. The three variants also showed high affinities toward the bacterial model system and drastically lost activity in the erythrocyte system (Table 2), making them visibly the most selective peptides (Fig. 3, *A* and *B*). In all cases, dose-response curves were adjusted with sigmoidal function.
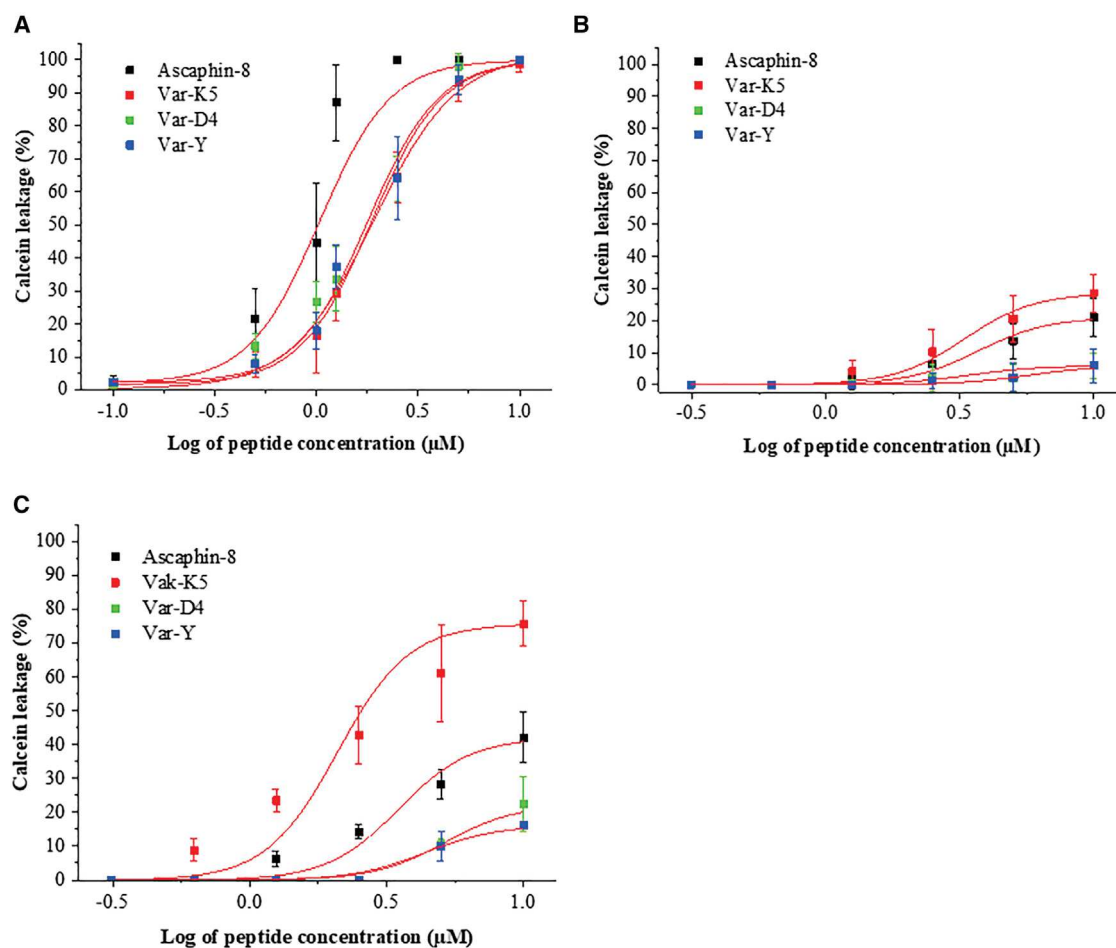

FIGURE 5 Calcein leakage induced by ascaphin-8 and its variants. (*A*) Dose-response curves of peptides against POPC:POPG (8:2) LUVs. (*B*) Dose-response curves of peptides against POPC:CHL (7:3) LUVs. (*C*) Dose-response curves of peptides against POPC:ERG (7:3) LUVs. To see this figure in color, go online.

TABLE 2 Effective concentrations (EC$_{50}$ and EC$_{80}$, μM) of ascaphin-8 and its variants against the bacterial, mammal, and fungal liposome models

Peptide	Bacterial model	Mammal model	Fungal model
EC$_{50}$ (μM)			
Ascaphin-8	0.986 ± 0.159	3.87 ± 1.10	3.54 ± 0.60
Var-K5	1.874 ± 0.217	3.58 ± 1.30	2.16 ± 0.33
Var-D4	1.745 ± 0.305	5.99 ± 2.15	4.97 ± 1.07
Var-Y	1.908 ± 0.397	6.18 ± 1.77	4.68 ± 0.87
EC$_{80}$ (μM)			
Ascaphin-8	1.717 ± 0.277	5.41 ± 1.54	5.38 ± 0.91
Var-K5	3.549 ± 0.334	5.01 ± 1.81	3.28 ± 0.50
Var-D4	3.039 ± 0.531	8.36 ± 3.01	7.54 ± 1.63
Var-Y	3.322 ± 0.691	8.63 ± 2.47	7.10 ± 1.33

In a study published by Eley et al. (20), five variants of ascaphin-8 were designed, whereby each amino acid on the hydrophilic face of the helix was replaced by L-lysine (K4, K8, K10, K14, and K18). All the analogs showed improved therapeutic indexes (i.e., potent antimicrobial activity but low hemolytic activity), except for K4 and K8, which also presented high hemolytic activity. The authors discussed that the general trend resulted from increased positive charge of the peptide-promoting interactions with negatively charged bacterial membranes, but not with the erythrocyte's neutrally charged CHL and zwitterionic phospholipids. In this study, although no substitutions were made, K3 and L5 positions were switched (see Fig. 1). Since the physicochemical properties were unchanged, the differences in behavior toward the different liposomal systems could be accounted for by the structural and spatial changes in the peptide as discussed earlier on (structure prediction and molecular dynamics, Figs. 2 and 3). On the other hand, although not related in structure, poly-L-lysines are known to be potent antimycotic agents, whereby they preferentially bind to mixed bilayers containing ERG over PC:CHL bilayers (63). However, we have no rational explanation for the behavior of the K5 variant toward the fungal model; moreover, there has not been a similar observation reported in the literature.

In the case of the Var-Y (F3Y; F19Y) variant, phenylalanines in positions 2 and 19 were replaced by tyrosine residues. Phenylalanine is more hydrophobic than tyrosine and, thus, the hydrophobicity and GRAVY values decreased (Table 1); the substitution of tryptophan by tyrosine has been observed to reduce drastically antibacterial activity (64–66). Similarly, the affinity of the Var Y variant decreased toward the sterol systems. However, hydrophobic peptide activity is enhanced in the presence of PC (67) and lipid membranes by extension (68). Generally, the polar-aromatic residues tryptophan and tyrosine have a specific affinity for a region near the lipid carbonyls (54), whereas phenylalanine can be found deeply inserted in bacterial and mammalian-mimic membranes (69). In this study, it can be argued that the increased selectivity (loss of activity toward systems with sterols) of the Var Y variant was a

direct consequence of the reduced hydrophobicity of the peptide, and reduced membrane penetration of tyrosine versus phenylalanine. Fluorescence and quenching experimental approximations could give insight on these assumptions.

Important to point out that the SVM peptide prediction tool was accurate because the order of affinity determined experimentally for the bacterial system is the same as the one predicted by this algorithm.

Effect of ascaphin-8 and its variants on membrane fluidity

The maintenance of membrane fluidity is essential for normal cell function (70). The extent of the molecular disorder and molecular motion within a lipid bilayer is defined as membrane fluidity (71). Several methods can be used to monitor membrane fluidity; however, the solvatochromic fluorophore Laurdan is one of the most popular, versatile, established probes used for studying this phenomenon (72). In addition, BA was used as a classical membrane fluidizer. Alcohols interact with lipid bilayers, with the -OH group positioned in the bilayer interfacial region and with the hydrocarbon chains facing the hydrophobic core of the bilayer modifying interaction between lipids in the system, membrane deformability, and fluidity (73). The results obtained from the changes in membrane fluidity induced by ascaphin-8 and its variants show that these peptides not only have the ability to form pores in lipid membranes but they also have the ability to modify membrane order (i.e., fluidity) (Fig. 6).

Although there were no significant differences among peptides, all the peptides induced membrane rigidity in the POPC:POPG membrane model (Fig. 6 A). On the other hand, none of the peptides induced observable changes in the POPC:CHL or POPC:ERG systems (Fig. 6, B and C). The difference in the ability of ascaphin-8 and its variants to induce changes in the bacterial model and not in the erythrocyte and fungal models (Fig. 6, C and D) may be related to the differences in affinity toward both models, as seen in the calcein leakage experiments (i.e., less efficient electrostatic interactions with the polar heads of the lipid molecules, and/or possibly comparatively low peptide insertion and pore formation rates.

Moreover, this difference in affinity could result from the physical nature of both systems. It is noteworthy that the bacterial model is considerably more fluid than the erythrocyte model. Thus, the much lower affinity may be because sterols, such as CHL and ERG, are known to act as a buffer and resist changes in membrane fluidity (74). Another interpretation is that lipid-peptide interactions are stronger in PC:PG membranes and that these interactions induce different lipid order in the system. MD simulations are a good option to evaluate the interaction of these peptides with the respective membranes in detail.